Available online at www.sciencedirect.com
SCIENCE DIRECT
Bioorganic & Medicinal Chemistry Letters 16 (2006) 1151–1155
Bioorganic & Medicinal Chemistry Letters

Synthesis and structure–activity relationships of novel pyrrolocarbazole lactam analogs as potent and cell-permeable inhibitors of poly(ADP-ribose)polymerase-1 (PARP-1)

Gregory J. Wells,* Ron Bihovsky,† Robert L. Hudkins, Mark A. Ator and Jean Husten

Cephalon, Inc., 145 Brandywine Parkway, West Chester, PA 19380-4245, USA

Received 5 October 2005; revised 24 November 2005; accepted 28 November 2005
Available online 15 December 2005

Abstract—A series of novel pyrrolocarbazole lactams was identified as potent PARP-1 inhibitors in vitro and in a PC12 cellular NAD^+ depletion assay. The SAR trends of substituents at the 3-position, as well as the effect of blocking the indole or lactam NH-groups of the template by methylation or formylation, are discussed in relation to molecular modeling studies.

Poly(ADP-ribose)polymerases (PARPs) comprise a family of proteins possessing poly(ADP)ribosylation activity and are involved in many aspects of cellular function and regulation. Six members of this family have been identified to date, the first discovered and best characterized being PARP-1 (EC 2.4.2.30), a 116 kDa chromatin-bound nuclear enzyme intimately involved in DNA replication and repair, telomerase activity, and cytoskeletal activity.[1] Ongoing studies continue to reveal evidence implicating PARP-1 in an ever wider known range of nuclear processes and gene activities affecting many physiological and developmental pathways.[2]

Though normal PARP-1 activity appears primarily to facilitate repair of DNA damage resulting from typical metabolic or environmental factors, its overactivation due to severe genotoxic stressors (e.g., ischemia, shock, diabetes, myocardial infarction, ionizing radiation, and alkylating agents) leads to excessive energy (ATP) depletion and ultimately necrotic cell death. Thus, potent and specific PARP-1 inhibitors may provide a therapeutic option for a variety of CNS disorders or traumatic injury. Inhibitors of PARP-1 may also have therapeutic utility in adjuvant cancer therapy with alkylating agents and/or radiation by suppressing DNA repair and driving tumor cells into apoptosis.[3]

A variety of PARP-1 inhibitors have been reported in recent years, nearly all being competitive with NAD^+, typically nicotinamide or aminobenzamide analogs.[4] Screening of our internal chemical library identified a pyrrolocarbazole template possessing an imide or lactam A-ring as potent PARP-1 inhibitors (Fig. 1).[5] Subsequent structural modifications around this template identified key elemental features that define the minimal pharmacophore essential for PARP-1 inhibition.[6] Discussed in this paper are the synthesis and SAR of lactam analogs with varying functionality at the 3-position and nitrogen atoms of the pyrrole C-ring and lactam A-ring.

To aid our structure-based design strategy toward the development of more potent inhibitors around this template, a molecular docking study was conducted.

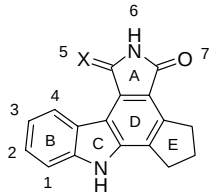

1
(X = H,H; O)

Figure 1. Pyrrolocarbazole template and numbering scheme.

Keywords: Poly(ADP-ribose)polymerase; Pyrrolocarbazole; Lactam; DNA repair; Cancer.
* Corresponding author. E-mail: gwells@cephalon.com
† Present address: Key Synthesis LLC, 804 Primrose Lane, Wynnewood, PA 19096, USA.

0960-894X/$ - see front matter © 2005 Elsevier Ltd. All rights reserved.
doi:10.1016/j.bmcl.2005.11.086

The refined crystal structure for the C-terminal catalytic fragment of chicken PARP (PARP-CF) in complex with PARP-1 inhibitors has been reported.[7] PARP-CF displays 87% sequence homology with its respective human counterpart. A binding model for PARP-1 was derived using the coordinates for 4-amino-1,8-naphthalimide bound at the NAD^+ site of the catalytic domain (PDB code = 2PAX) at a resolution of 2.4A.[8] Adapting this model for the design of inhibitors around our carbazole template, compound **9** was docked and minimized at the NAD^+ site of PARP-CF (Fig. 2). Key H-bond interactions were observed between the lactam C=O and NH groups and backbone Gly863 NH and O, a H-bond between the indole NH group and C=O of the Glu988 side chain, and favorable aromatic π-stacking interactions of the aryl rings of Tyr896 and Tyr907 with the B and D rings of the carbazole, respectively. The cyclopentyl ring fits closely into a fold formed by the Lys861 side chain, Ala898, Trp861, and Asn987. An open pocket was observed around the 3- and 4-positions, providing an apparent opportunity for structural modifications in this region and the rational development of SAR for this structural class of molecules, as discussed below.

The synthesis of pyrrolocarbazole lactams and related analogs is shown in Schemes 1–3. The key diene intermediate, **3**, was prepared by sequential deprotonation of indole (**2**) with *n*-BuLi followed by treatment with carbon dioxide to mask the indole nitrogen. Removal of excess CO_2 followed by treatment with *t*-BuLi and cyclopentanone at low temperature gave the tertiary alcohol, which was dehydrated with hydrochloric acid at room temperature to give **3**. Diels–Alder reaction of this diene with *cis*-ethyl-3-cyanoacrylate in chlorobenzene at 125 °C gave a diastereomeric mixture of two nitrile-ester regioisomers, **4** and **5**, which were separated by column chromatography and subsequently treated with DDQ in toluene at 60 °C to give the oxidized regioisomers **6** and **7**. The cyanoesters were treated with hydrogen (50 psi) and Raney nickel in DMF, leading to reduction of the nitrile and spontaneous cyclization in situ to give lactams **8** and **9**. Halogenation of **9** with NCS or NBS gave the corresponding 3-halo derivatives, **10** and **11**, respectively. Treatment of bromide **11** with excess zinc cyanide mediated by tetrakis-(triphenylphosphine)-palladium(0) catalysis in refluxing DMF gave nitrile **12**. Reduction of the nitrile to the aminomethyl analog, **13**, was achieved by hydrogenation over Raney nickel. Alternatively, nitrile **12** could be hydrolyzed to carboxylic acid **15** with hydrochloric acid and 1,4-dioxane. Treatment of **15** with TMS–diazomethane gave methyl ester **16**. Amine **13** and carboxylic acid **15** were converted to amide analogs, **17a**–**17h**, by treatment with carboxylic acids or amines, respectively, using standard HOBt/BOP coupling methodology. Treatment of Boc-protected lysyl analog, **17h**, with hydrochloric acid and 1,4-dioxane at ambient temperature gave the free diamino analog, **17i**. Preparation of the 3-methyl analog **14** was accomplished by treatment of bromide **11** with Me_4Sn and catalytic tetrakis-(triphenylphosphine)palladium(0) in DMF. Alkylation of **9** with NaH and methyl iodide gave a mixture of mono- and di-*N*-methyl analogs, **18** and **19**, which were separated by conventional flash chromatography on silica gel. Attempted Vilsmeier–Haack formylation of **9** gave the *N*-formyl analog, **20**, instead as the exclusive product.

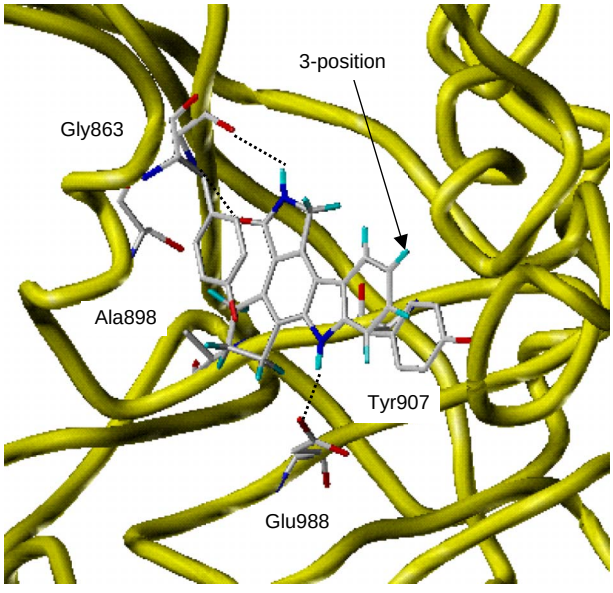

Figure 2. Compound **9** docked to PARP-CF.

The compounds prepared in this study were evaluated as inhibitors of recombinant human PARP-1.[9] As shown in Table 1, it quickly became clear that the 5-oxopyrrolocarbazole (**8**) was inactive (>10 μM), while the 7-oxopyrrolocarbazole (**9**) was nearly equipotent to the corresponding imide analog (**21**)[5] (56 nM vs 36 nM, respectively), illustrating the importance of the 7-oxo group for binding to the active site, as suggested by our modeling studies.

As shown in Table 2, the bromo and cyano analogs, **11** and **12**, displayed moderately improved in vitro potency relative to parent compound **9**, suggesting that steric bulk and electron-withdrawing groups are well tolerated at this position. Aminomethyl analog, **13**, also showed good potency (27 nM), while, curiously, the 3-methyl analog **14** was significantly less active. *N*-Methyl analogs **18** and **19**, along with the *N*-formyl analog, **20**, were very weakly active, confirming an essential role for both NH-groups for activity and further supporting our modeling work. Thus, a series of amino- and heterocyclic-containing amides of **13** and **15** were prepared in an effort to improve both potency and water solubility, and physico-chemical properties of this otherwise poorly soluble template.

(Dimethylamino)ethyl- and (morpholin-4-yl)ethyl-amides (**17a**, **17b**) displayed decreased activity, as did the ethylene- or methylene-linked pyrid-2-yl, imidazol-4-yl, and triazole-1-yl analogs (**17e**, **17f**, and **17g**). Potency was somewhat restored by incorporation of the shorter-chain morpholin-4-yl-amide (**17c**, 83 nM) or the isomeric (to **17e**) pyrid-4-yl analog, **17d** (65 nM). The di-*N*-Boc-lysyl-bearing analog, **17h**, was only

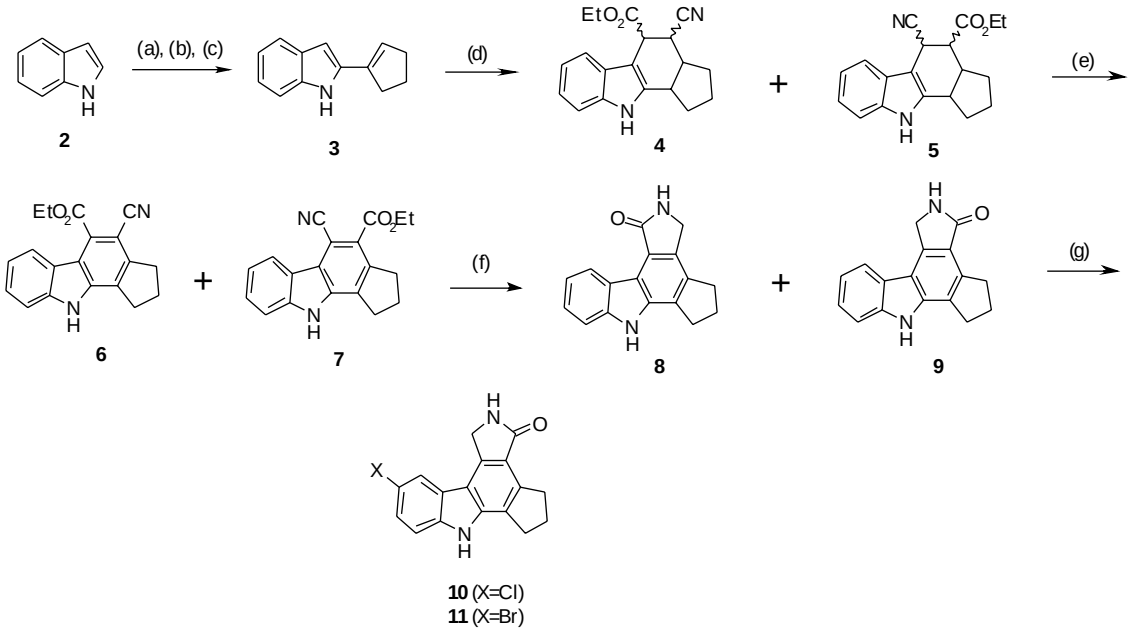

Scheme 1. Reagents and conditions: (a) *n*-BuLi, THF, −78 to +20 °C, then CO_2(g); (b) *t*-BuLi, THF, −78 °C, then cyclopentanone; (c) 2 M HCl, acetone, rt; (d) *cis*-$EtO_2CCH{=}CHCN$, PhCl, 125 °C; (e) DDQ, toluene, 60 °C; (f) H_2, Ra-Ni, DMF, rt; (g) NCS or NBS, DMF, rt.

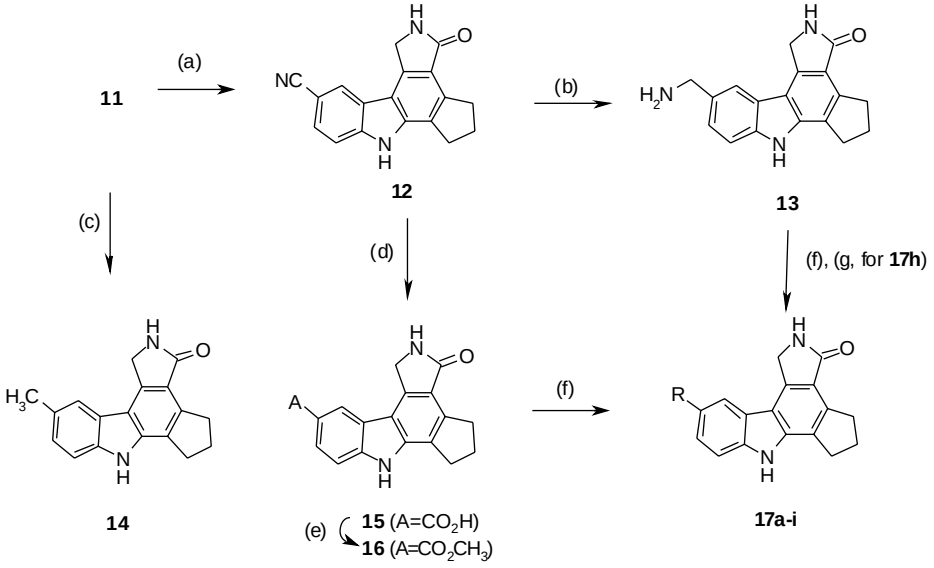

Scheme 2. Reagents and conditions: (a) $Zn(CN)_2$, $Pd(Ph_3P)_4$, DMF, 130 °C; (b) H_2, Ra-Ni, DMF, MeOH, rt; (c) Me_4Sn, $Pd(Ph_3P)_4$, DMF, 130 °C; (d) concd HCl, 1,4-dioxane, 100 °C; (e) $TMSCHN_2$, hexanes, EtOH, DMF, rt; (f) R^1R^2NH (for **15**) or RCO_2H (for **13**), HOBt, BOP, NMM, DMF, 20–65 °C; (g) 2 M HCl, 1,4-dioxane, rt.

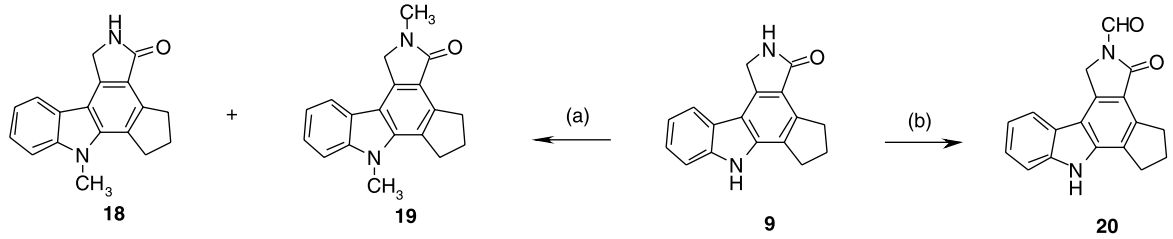

Scheme 3. Reagents and conditions: (a) MeI, NaH, DMF, rt; (b) DMF, $POCl_3$, rt.

Table 1. PARP-1 activity of related pyrrolocarbazole lactam and imide analogs

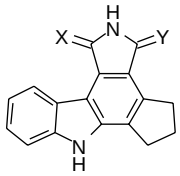

Compound	X	Y	IC_{50} (nM)
8	O	H, H	>10,000
9	H, H	O	56
21	O	O	36

weakly active (670 nM), while its deprotected analog, **17i**, was relatively potent (80 nM).

The depletion of NAD^+ pools following oxidative injury has been correlated to PARP activation.[10] The inhibition of NAD^+ depletion following hydrogen peroxide insult in PC12 cells was utilized to assess the cell permeability of compounds.[11] The ability of compounds to attenuate the decrease in NAD^+ levels was examined and the results were normalized to the maximal effect of a reference compound at 30 μM (5*H*-phenanthridin-6-one[12]). The NAD^+ levels are reported as % recovery as compared to untreated cells. The cell % NAD^+ recovery at 1 μM was used as an index of potency, while the maximal recovery at 30 μM reflects the efficacy (Table 2).

Although parent compound **9** showed good cellular activity (48% NAD^+ recovery at 1 μM), the maximal recovery was only 68% at 10 μM and is probably limited by its poor aqueous solubility (≪0.001 mg/mL). In contrast, the aminomethyl analog, **13**, showed similar potency (39% NAD^+ recovery at 1 μM) with much better efficacy (102% NAD^+ recovery at 30 μM) than any of the other amide analogs studied in this series. Thus, with compound **13**, significantly improved aqueous solubility (∼0.1 mg/mL), high in vitro potency, and good cellular activity have all been achieved concurrently in the same molecule.

In summary, we have identified a series of novel pyrrolocarbazole lactams as potent PARP-1 inhibitors. Molecular modeling studies revealed essential H-bonding interactions of both indole and lactam NH-groups within the active site of the enzyme, which was supported experimentally by methylation (or formylation) at these positions, leading to inactive analogs. An open pocket near the active site, corresponding to the 3- and 4-positions of the carbazole template, allowed development of an SAR around this region and led to analogs with good in vitro potency, aqueous solubility, and activity in a PC12 cellular assay. Future progress in this area will hinge on identifying molecules with ade-

Table 2. PARP in vitro and cellular activity of 3-substituted pyrrolocarbazole lactams

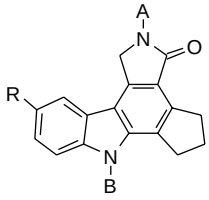

Compound	A	B	R	PARP-1 IC_{50} (nM)[a]	Cell % NAD^+ recovery	
					at 1 μM[a]	at 30 μM
9	H	H	H	56	48	68[b]
10	H	H	Cl	120	26	133
11	H	H	Br	30	28	47[b]
12	H	H	CN	18	26	74[b]/122
13	H	H	CH_2NH_2	27	39	102
14	H	H	CH_3	200	17	50
15	H	H	CO_2H	80	24	65
16	H	H	CO_2CH_3	59	38	134
17a	H	H	CONH–$(CH_2)_2$–$N(CH_3)_2$	165	6	36
17b	H	H	CONH–$(CH_2)_2$–morpholin-4-yl	162	7	27
17c	H	H	CO–morpholin-4-yl	83	18	74
17d	H	H	CON(CH_3)–CH_2–pyrid-4-yl	65	23	101
17e	H	H	CON(CH_3)–CH_2–pyrid-2-yl	237	11	44
17f	H	H	CON(CH_3)–$(CH_2)_2$–imidazol-4-yl	161	5	39
17g	H	H	CONH–$(CH_2)_2$–triazol-1-yl	105	12	28
17h	H	H	CH_2NHCOCH–(NHBoc) [$(CH_2)_4$NHBoc]	670	ND	ND
17i	H	H	CH_2NHCOCH(NH_2) [$(CH_2)_4NH_2$]	80	2	48
18	H	CH_3	H	800	ND	ND
19	CH_3	CH_3	H	10,000	ND	ND
20	CHO	H	H	3000	ND	ND

ND, not determined.

[a] Values of duplicate determinations for 20 compounds are within 2-fold of each other.

[b] % NAD recovery at 10 μM.

quate PK/PD properties and, ultimately, in vivo activity in a clinically relevant model.

Acknowledgments

The authors express their appreciation to Drs. John P. Mallamo and Jeffry L. Vaught for useful discussions and suggestions.

References and notes

1. (a) Yu, S.-W.; Wang, H.; Poitras, M. F.; Coombs, C.; Bowers, W. J.; Federoff, H. J.; Poirier, G. G.; Dawson, T. M.; Dawson, V. L. *Science* **2002**, *297*, 259; (b) D'Amours, D.; Desnoyers, S.; D'Silva, I.; Poirier, G. G. *Biochem. J.* **1999**, *342*, 249; (c) Smith, S. *Trends Biochem. Sci.* **2001**, *26*, 174.
2. (a) Ju, B.-G.; Solum, D.; Song, E. J.; Lee, K.-J.; Rose, D. W.; Glass, C. K.; Rosenfeld, M. G. *Cell* **2004**, *119*, 815; (b) Kim, M. Y.; Mauro, S.; Gevry, N.; Lis, J. T.; Kraus, W. L. *Cell* **2004**, *119*, 803; (c) Tulin, A.; Spradling, A. *Science* **2003**, *299*, 560.
3. (a) Virag, L.; Szabo, C. *Pharmacol. Rev.* **2002**, *54*, 375; (b) Bryant, H. E.; Helleday, T. *Biochem. Soc. Trans.* **2004**, *32*(P6), 959; (c) Skaper, S. D. *Curr. Drug Targets: CNS Neurol. Disord.* **2003**, *2*, 279; (d) Tentori, L.; Leonetti, C.; Scarsella, M.; d'Amati, G.; Portarena, I.; Zupi, G.; Bonmassar, E.; Graziani, G. *Blood* **2002**, *15*, 2241; (e) Miknyoczki, S. J.; Jones-Bolin, S.; Pritchard, S.; Hunter, K.; Zhao, H.; Wan, W.; Ator, M.; Bihovsky, R.; Hudkins, R.; Chatterjee, S.; Klein-Szanto, A.; Dionne, C.; Ruggeri, B. *Mol. Cancer Ther.* **2003**, *2*, 371; (f) Delaney, C. A.; Wang, L. Z.; Kyle, S.; White, A. W.; Calvert, A. H.; Curtin, N. J.; Durkacz, B. W.; Hostomsky, Z.; Newell, D. R. *Clin. Cancer Res.* **2000**, *6*, 2860.
4. (a) Beneke, S.; Diefenbach, J.; Burkle, A. *Int. J. Cancer* **2004**, *111*, 813; (b) Stefan, P.; Schwahn, U. *Exp. Opin. Ther. Pat.* **2004**, *14*, 1531; (c) Soldatenkov, V. A.; Potaman, V. N. *Curr. Drug Targets* **2004**, *5*, 357; (d) Pellicciari, R.; Camaioni, E.; Costantino, G. *Prog. Med. Chem.* **2004**, *42*, 125; (e) Nguewa, P. A.; Fuertes, M. A.; Alonso, C.; Perez, J. M. *Mol. Pharmacol.* **2003**, *64*, 1007.
5. Ator, M. A.; Bihovsky, R.; Chatterjee, S.; Dunn, D.; Hudkins, R. L.; WO Pat. 01/85686 A2, 2001.
6. Tao, M.; Park, C. H.; Bihovsky, R.; Wells, G. J.; Husten, J.; Ator, M. A.; Hudkins, R. L. *Bioorg. Med. Chem. Lett.*, in press.
7. Ruf, A.; Menissier de Murcia, J.; de Muricia, G. M.; Schulz, G. E. *Proc. Natl. Acad. Sci. U.S.A.* **1996**, *93*, 7481.
8. Ruf, A.; de Murcia, G. M.; Schulz, G. E. *Biochemistry* **1998**, *37*, 3893.
9. PARP assays were carried out in 96-well filter plates (Millipore, MADP NOB 50) in a final volume of 100 μL in 100 mM Tris, pH 8.0, 2 mM DTT, 10 mM $MgCl_2$, and 20 μg/mL DNA (nicked by sonication), 20 μg/mL H1 (histone), and 100 μM NAD^+, supplemented with 2 μCi [^{32}P]NAD^+/mL. The human PARP concentration was 50 ng/mL. Following a 10 min reaction at room temperature, the protein was precipitated with TCA, washed, and the radiolabeled product was quantified by scintillation counting. Banasik, M.; Komura, H.; Shimoyama, M.; Ueda, K. *J. Biol. Chem.* **1992**, *267*, 1569; Panzeter, P. L.; Zweifel, B.; Althaus, F. R. *J. Chromatogr., A* **1994**, *678*, 35.
10. Heller, B.; Wang, Z.-Q.; Wagner, E. F.; Radons, J.; Burkle, A.; Fehsel, K.; Burkart, V.; Kolb, H. *J. Biol. Chem.* **1995**, *270*, 11176.
11. PC12 cells were plated onto polyornithine/laminin-coated 96-well plates. Prior to addition of inhibitors, growth medium was replaced with low serum medium. Cells were pre-treated for 1 h with PARP inhibitors, then with 0.5 mM hydrogen peroxide for 30 min in the presence of inhibitors. After washing away the peroxide, fresh PARP inhibitors were added. One hour after peroxide treatment the cell surface was washed once with phosphate-buffered saline. NAD^+ was released into phosphate-buffered saline by subjecting the cells to two freeze/thaw cycles. After centrifugation, the supernatant was analyzed for NAD^+ using the method described in Shah, G. M.; Poirier, D.; Duchaine, C.; Brochu, G.; Desnoyers, S.; Lagueux, J.; Verreault, A.; Hoflack, J. C.; Kirkland, J. B.; Poirier, G. G. *Anal. Biochem.* **1995**, *227*, 1.
12. Banasik, M.; Komura, H.; Shimoyama, M.; Ueda, K. *J. Biol. Chem.* **1992**, *267*, 1569.